Environ Earth Sci
DOI 10.1007/s12665-011-1015-y

ORIGINAL ARTICLE

Importance of porosity and transfer of matter in the rock weathering processes: two examples in central Spain

E. Molina Ballesteros · J. García Talegón · A. C. Iñigo Iñigo · M. González Sánchez · H. Herrero Fernández

Received: 31 March 2009 / Accepted: 14 February 2011

Abstract Some physical properties (bulk and free porosity, pore size distribution), and the chemical composition and mass balance of two deeply weathered profiles one developed on Hercynian granodiorite and the other on pre-Cambrian slates were studied. Hydric and mercury porosimetry, nitrogen adsorption techniques, chemical analyses and XRD techniques were used. On granodiorite, weathering has created increased porosity with a pore diameter <5 µm, whereas on slates the weathering has produced of ca. 1 µm in diameter. These pore sizes have played an important role in the weathering processes. Assuming that weathering preserves volumes, except in the uppermost part of the profiles, it brought about a loss of matter of more than 12% (~300 kg/m^3) on granodiorite and ca. 30% (~800 kg/m^3) on slates. These changes are related to shifts in the mineralogical evolution, with the appearance of new 2:1 and 1:1 phyllosilicates and Fe oxy-hydroxides as the main authigenic minerals. The release of matter, at least since the upper Neogene until the present, has led to the lowering of relief in a more or less homogeneous way, giving rise to gentle hillsides and flat surfaces below which the current river networks are incised. Porosity studies have the potential to explain several specific landforms as well as affecting landscape development in general.

Keywords Weathering · Porosity · Mass balance · Granodiorite · Slates · Piedmont surfaces

Introduction

The oldest geological entity of the Iberian Peninsula is the Hercynian basement which crops out in the western half (Fig. 1a). It is formed of the rocks affected by and generated during the Hercynian orogeny, some 305 Ma. ago. During the Mesozoic and early Cainozoic, this basement underwent long cycles of erosion (Swenzner 1936; Ribeiro 1942; Solé Sabaris 1952; Gladfelter 1971; Martín Serrano 1988) leading to the development of extensive erosion surfaces (the "fundamental polygenic peneplain" of Pedraza 1978) and to residual mountain ranges (such as the Montes de Toledo, Sierra Morena, etc.), and inselbergs in resistant lithologies standing up to 200–400 m above the planation surface. Remnants of this old relief are preserved in horsts and grabens elevated by the Tertiary Alpine orogeny which thus fundamentally changed the reginal topography (Birot and Solé Sabaris 1954; Portero and Aznar 1984; Martín Serrano 1991; Cantano Martín and Molina Ballesteros 1999).

Erosion of these reliefs produced a sedimentary cover named the Raña which is widely distributed over the basement rocks. Rañas are piedmont deposits up to 20 m thick in the scarp foot but less than a metre thick in the distal zones. They are formed of pebbles, gravels and sands embedded within a clayey matrix of reddish to ochre hues. Morphologically, they form piedmont platforms (Fig. 1b)

E. Molina Ballesteros (✉) · J. García Talegón
Dpto. de Geología, Universidad de Salamanca, Salamanca, Spain
e-mail: emoli@usal.es

A. C. Iñigo Iñigo · M. González Sánchez · H. Herrero Fernández
Insto. de Recursos Naturales y Agrobiología de Salamanca (IRNASA-CSIC), Salamanca, Spain

E. Molina Ballesteros · J. García Talegón · A. C. Iñigo Iñigo · M. González Sánchez · H. Herrero Fernández
Unidad Asociada de Investigación Universidad de Salamanca-CSIC, Salamanca, Spain

Published online: 29 March 2011

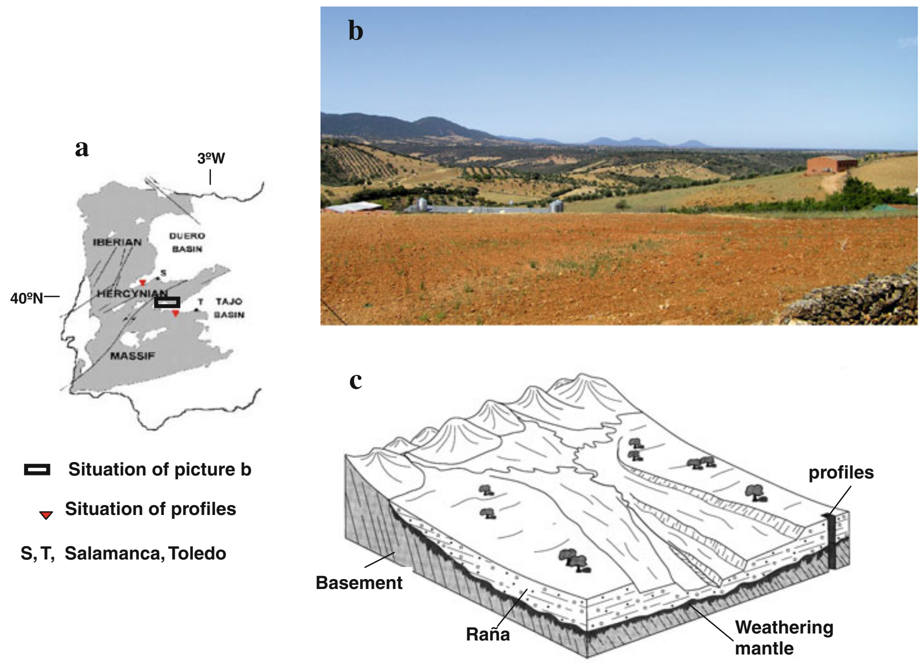

Fig. 1 **a** Map of the Iberian Hercynian Massif and situation of the picture **b**. **b** typical view of the Raña piedmont eroded by the rivers coming from the Montes de Toledo, near Los Navalucillos village. **c** Sketch of a Raña landscape with the position of the weathering mantle beneath the Raña cover

sloping gently (ca. 1–2%) from the scarp foot to the axes of the local drainage basins, the main rivers of which (e.g. Tajo, Duero) are more than 150 m lower down. The age of the Raña cover is unresolved, but an age-range from the Upper Neogene to the earliest Pleistocene can be assumed.

Beneath these piedmont deposits, the outcrops of the basement are consistently weathered to a considerable depth (Fig. 1c). Slates, migmatites, granitoids, quartzites, etc. and all types of dykes are affected by a weathering mantle 50 m or more thick, the degree of weathering increases upwards within the sequence. This type of profile is characteristic of the central "Meseta" of the Iberian Peninsula.

Many profiles developed on this sedimentary cover have been studied from a pedological viewpoint, paying attention to mineralogical and/or agronomic aspects (Espejo 1978, 1987; Vaudour 1977; Gallardo et al. 1987; Martín Serrano 1988; Ingelmo et al. 1991; Pardo et al. 1993; Martínez Lope et al. 1995; Molina et al. 1991; Molina Ballesteros and Cantano Martín 2002). In the Montes de Toledo region (provinces of Ciudad Real and Toledo, central Spain), the study of such weathering profiles cropping out beneath the Raña were studied by authors as Vicente et al. 1991, 1997; Borger 1997; Clausell et al. 2001. All these works have yielded the following general conclusions:

– The sediments of the Raña are palaentological deserts for they are unfossiliferous, with the exceptions of fragments of quartzites which are transported from the headwater regions and which include the imprints of trilobites.
– The main types of soil developed on the Raña are luvisols, ultisols and planosols with local formation of vertisols. Profiles are rich in clay (up to ca. 50% in some horizons) with a more-or-less acid trend, hydromorphic features, significant changes in internal structure, and migration of matter and ions (mainly of Si, Al and Fe) through the profile.
– The three zones are developed in the weathered basement: (1) a lower level, with the inherited parent mineralogy; (2) an intermediate level in which there is bisialitization (generation of phyllosilicates 2:1), and (3) an upper level, where monosialitization (generation of phyllosilicates 1:1) has occurred.
– The same weathering processes have affected both the sedimentary cover and the basement, but under different conditions. The changes look like similar to toposequences developed under tropical and subtropical climates.

The work reported here is concerned not with the weathering process, but with changes in porosity, density, and transfer of matter that have affected the uppermost parts of the basement beneath these covers. Two profiles, one developed on a two-mica granodiorite and the other on slates, and both outcropping under the Raña cover are analysed and discussed.

The first profile is located in the province of Toledo (Fig. 1 a), cropping out on a 70 m high scarp of along the road between the towns of Navahermosa and Los Navalmorales, close to the resort “Urbanización Rio Cedena” (URC) (39°39′29″N; 4°32′14″W), in the northern piedmont of the Montes de Toledo. It stands at an elevation of ca. 770 m a.s.l.. The region has a Mediterranean climate with a continental trend but influenced by the nearby mountains with summits between 1,200 and 1,400 m high. The mean annual temperature measured in the villages located in the piedmont is 14°C (e.g. Navahermosa, mean January 4°C, July 26°C). The annual rainfall in the zone varies between 500 mm in the piedmont up to >900 mm in the summits of the mountains where snow may settle for some weeks during January or February. The water balance of these soils shows a deficit from May to September or October, and a surplus of water (22–35%) from January to April (Espejo 1978).

The second site is located in the southwestern border of the Duero basin and close to the Portuguese border (province of Salamanca, western Spain). The Alpine orogeny gave rise to the elevated bloc of the sierras Tamames–Francia to the south, and the Ciudad Rodrigo basin, with a NE–SW trend, to the north (Fig. 1). From these sierras, an apron of alluvial fans extends into the basin forming the Rañas of this region. The profile studied is located at ca. 1060 m a.s.l., at the intersection of the roads joining the villages of Serradilla (SER), El Maillo and Morasverdes (40°33′56″N; 6°12′05″W) on a scarp some 70 m high. There have been previous investigations of the soils of the Raña (García Rodríguez et al. 1977; García Rodríguez 1987; Ingelmo et al. 1991; Molina Ballesteros and Cantano Martin 2002), and of the weathered basement rocks beneath (Molina et al. 1990; Cantano Martín M (1996) Evolución morfodinámica del sector suroccidental de la cuenca de Ciudad Rodrigo. Salamanca. Tesis Doctoral, Univ. Huelva, unpublished).

The region has a Mediterranean climate affected by the mountains located just to the south with summits more than 1700 m a.s.l. Oceanic influences are introduced from the west along the Ciudad Rodrigo basin. Mean annual temperature also varies between <10°C in the mountains up to ca. 13°C in the basin (Morasverdes, mean January 3°C, mean July 24°C). The annual precipitation (rainfall + snow) varies from ca. 500 mm in the interior of the basin up to >1300 mm in the highest points of the mountains. The water regime of these soils is something different to that of the Montes de Toledo (Ingelmo et al. 1991). The dry season is normally from June to September, with a water deficit <20% in soils close to the sierras and ca. 30% in soils located in the middle of the basin.

Overall runoff from the Raña soils can vary between ca. 20–45% of the rainfall, the highest being during winter (García Rodríguez et al. 1977; Espejo 1978; García Rodríguez 1987; Gallardo et al. 1987; Ingelmo et al. 1991; Pardo et al. 1993).

Materials, methods and techniques

Materials

The URC profile (Fig. 2) shows a lower part, of ca. 55–60 m high where a two-micas granodiorite outcrop is separated into blocks grading to corestones which are embedded in a light grey (10Y 7/1), massive and friable regolith. The upper part is formed of some 12–14 m of the Raña cover, with reddish (2.5YR 5/8) and yellow (2.5Y 7/8) hues and in which some sedimentary structures can be recognized. The granodiorite consists of crystals of quartz, K feldspars, plagioclases (of some centimeters long) and two micas as the main minerals.

The SER profile (Fig. 3) displays a lower section, where outcrops of Precambrian slates separated into slabs of grey hues (10Y 5/1), changing upwards first to orange (2.5YR 6/2) and then into a compact clayey mass of red hue (10R 4/8) crossed by yellowish (7.5YR 7/8) and light grey (10YR 8/2) ribbons, all beneath a structureless 2–3 m thick Raña cover.

In both profiles, the contact between the weathered basement and the Raña is erosional. But, whereas the inherited structures of the slates can be identified a few meters beneath the cover (Fig. 4), on granodiorite the weathering is some tens of meters deep and original structures are not apparent immediately beneath the sedimentary cover (Fig. 5). However, intrusive veins (quartz, pegmatites, etc.) are preserved their directions practically throughout the long of the profiles.

Methodology

To measure the degree of rock weathering, different methods have been developed, based on the changes in densities between weathered and non-weathered parent material, and/or assuming that during weathering some elements are not removed. Thus, some indices and numerical models based on mass-balance calculations have been developed (e.g. Reiche 1943; Parker 1970; Grant 1986; Brimhall et al. 1991; Baumgartner and Olsen 1995; Chiquet et al. 2000).

Referring to the silicate rocks, one of the geochemical indices used to measure the degree of weathering is the relationship between the acid ($SiO_2 + Al_2O_3$) and the alkaline and alkaline-earth ($CaO + MgO + Na_2O + K_2O$) components. It is based on the assumption that this relationship increases by the release of the latter during weathering.

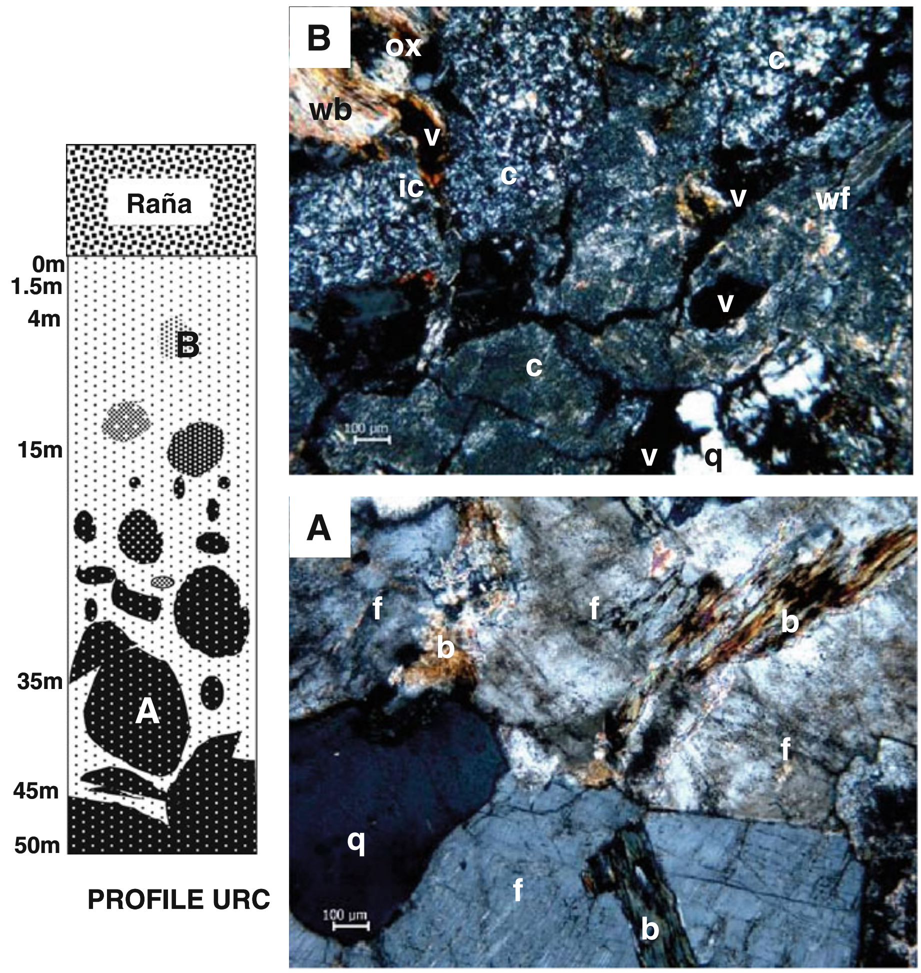

Fig. 2 Sketch and microphotographs (2 nicols) of thin sections of two samples from the URC profile. The no weathered corestones at the base of the profile (sample A) develop upward to arenized granodiorite (sample B) embedded into a sandy mass more or less rich in clays. Mineralogy of microphotographs: *q* quartz, *f-wf* feldspar more or less weathered, *b-wb* biotite more or less weathered, *c* clayey mass generated in situ by weathering (of feldspars?), *ox* Fe oxyhydroxides, *ic* illuviated clay, *v* voids. *Scale bar* 100 µm

Moreover, authors use many other relationships depending on the goal to outline.

Depending on the purpose of investigation other authors have used other methods, but taking into account the data obtained in this work, we decided to use both the mass-balance methods (e.g. Grant) and the method based on chemical calculations (e.g. Parker index). The relationships ($Al_2O_3 + Fe_2O_3$) to SiO_2, and K_2O to ($CaO + MgO + Na_2O$) were also applied in order to highlight some significant changes through the profiles.

Parker's index I_w (1970) was designed to point out the "capacity" or "facility" of a homogeneous rock to be weathered. It has mainly been used for igneous rocks, obtaining values of $I_w > 100$ for non-weathered basic and ultra basic rocks, and $I_w < 70$ for non-weathered leucocratic rocks. An increase in weathering leads to a reduction in the I_w index.

To ascertain how the major elements have moved throughout the profiles, the criteria of Grant (1986), based on the relationship between chemical composition and changes in the mass balance, were used. Grant's equation is:

$$C_i^A = \frac{M^O}{M^A}(C_i^O + \Delta C_i) \qquad (1)$$

where C_i^A and C_i^O are the concentrations of the component "*i*" in weathered (A) and non-weathered (O) parent rock, M^O and M^A are the masses of non-weathered and weathered rock, and ΔC_i is change in concentration of "*i*" due to weathering.

This is a function of a straight line (isocone) in a C_i^A versus C_i^O diagram in which M^O/M^A is the slope of the isocone.

Techniques

The mineralogy of the samples from the profiles was determined by:

- Observation of thin sections using a Leitz Laborlux 12 Pol S petrographic microscope.
- X-ray diffraction (XRD) on a Philips PW-1730 device with a PW-1050/81 goniometer, and a PW-1710

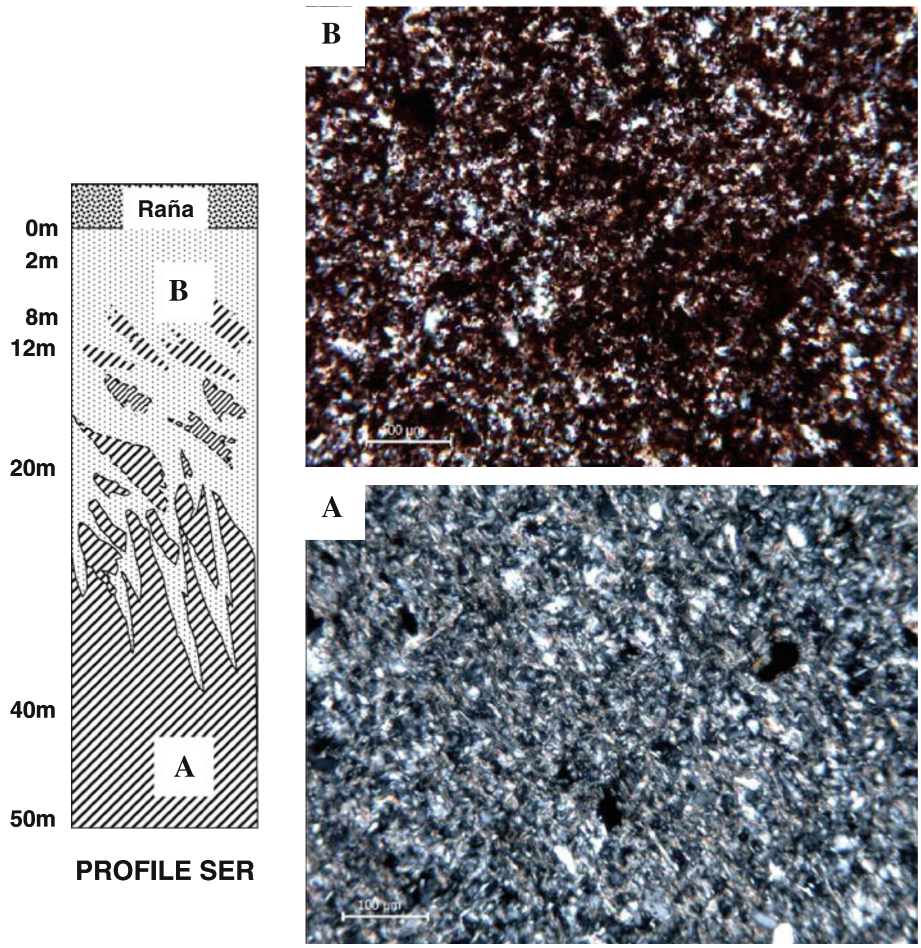

Fig. 3 Sketch and microphotographs (2 nicols) of thin sections of two samples from the SER profile. The unweathered slate (sample A) is rich in phyllosilicates, with some opaque minerals and grains of quartz (*white spots*). Most of the dark domains in microphotograph B (*weathered slate*) are Fe oxyhydroxide concentrations. *Scale bar* 100 μm

Fig. 4 View of the Raña cover, of no more than 4–5 m thick, upon the weathered slates in the surrounding of Serradilla del Arroyo. Pebbles and gravels of quartzite and some quartz are spread from the upper surface on the riverbanks and gullys

Fig. 5 Clear contact between weathered granodiorite and the Raña cover at the top of the URC profile. The regolith of the granodiorite is very soft and friable and the Raña displays some sedimentary structures in its lower parts

diffractometer control. XRD patterns of the <2 mm and <2 μm fractions for each sample, combining the powder and oriented aggregates methods. Moreover, the ethylene glycol and thermic treatments have been applied to the <2 μm fraction.

The petrophysical properties of the samples were studied using:

- Hydric determinations, providing information on changes in density and porosity, as indicated by French Standard Norms NF B10-503 (1973) and NF B10-504 (1973),
- Mercury porosimetry techniques, on a Quanta Chrome device, model PoreMaster PM 60-6, to determine pore size distribution and total porosity,
- Nitrogen adsorption–desorption isotherms of the samples by means of a Gemini apparatus from Micromeritics to know the specific surface, using a computer program developed by Rives (1990).

Major chemical elements were analyzed by emission spectrophotometry (IPC MASS) on a Pelkin Elmer apparatus after acid dissolution of the samples (HNO_3 + HF) by microwave digestion.

Results

Profile on Granodiorite

In the profile developed on granodiorite (Fig. 2), the many intrusive veins within the regolith showing that the section is in situ. The rocks of which they are composed become friable 1–2 m below the base of the Raña (Fig. 5). This means that most structures of the parent rock are preserved despite changes in rock density.

The hydric properties of the samples studied (Figs. 6, 7) show that weathering has not led to changes in real density but rather to a moderate reduction in bulk density (Fig. 6). Slight differences between total and free porosity upwards (Fig. 7) through it was not possible to measure in the uppermost part of the profile (1.5 m) as samples collapsed under water. The Hg porosimetry (Fig. 8) also revealed the increase in porosity upwards, showing that in samples from non-weathered granodiorite (corestone) the Hg porosimeter had not detected a porosity of <5 μm in diameter. By contrast, at the top of the weathering profile, a massive saprolite of finer porosity has developed, with the appearance of two maxima in the histogram of pore distribution: one between 0.1 and 1 μm and the other ca. 20 μm in pore diameter.

Measurements of specific surface by means of the nitrogen adsorption–desorption isotherm method were only useful in samples from the uppermost two levels of the profile, which were between 10 and 12 m^2/gr, the rest of samples having values below the limits of detection of the instrument. By contrast, the Hg porosimetry method showed values between 1.5 and 4 m^2/gr for samples from the top of the weathered granodiorite, while samples from the lower levels revealed values <1 m^2/gr.

The mineralogical data from this profile (Table 1) show a progressive enrichment in phyllosilicates, mainly of the 1:1 (kaolinite *s.l.*) and 2:1 (smectite *s.l.*) groups, with a slight reduction in feldspars upwards. Moreover, Table 2 points out that there is an increase in both the acid/alkaline and in the $K_2O/(CaO + MgO + Na_2O)$ fractions above ca. 15 m deep.

Taking into account that the dykes, mainly of quartz, aplite and pegmatite, preserve their directions throughout almost the whole profile, we assume that weathering has been conservative in volume (isovolume). Thus, M^O and M^A of the Grant's Equation (1) can be replaced by the bulk densities ρ^O and ρ^A, respectively. Table 3 shows the values of ΔC_i for each component, and $\Sigma\Delta C_i$ is the matter lost by the different levels. Data of the Parker's index from the samples are also shown.

Profile on slates

In the profile on slates (Figs. 3, 4), one of the first traits of weathering is the development of splinters of 5–15 cm in length, their size shrinking upwards, this leading to a compact level of weathered slates in which some inherited structures are preserved (e.g. planes of diaclases), although the schistosity has been wiped out. The colours change from grey hues of the "no" weathered slates at the bottom, to reddish hues crossed by yellowish and bleached ribbons

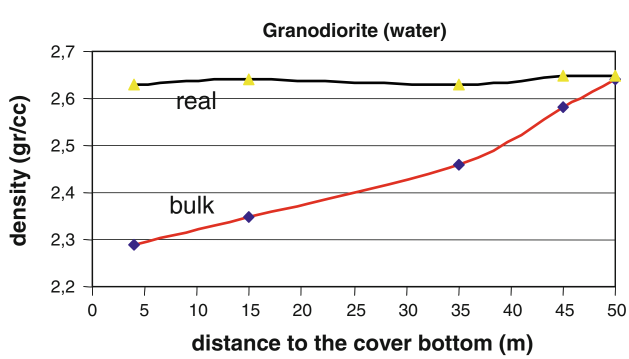

Fig. 6 Changes in real and bulk densities with depth in the URC profile

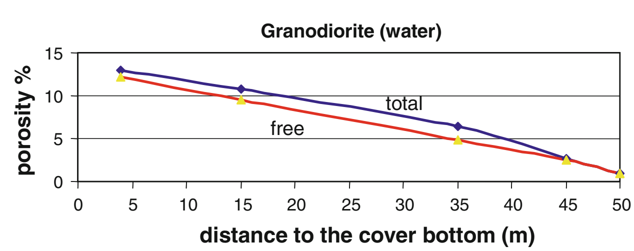

Fig. 7 Changes in total and free porosities with depth in the URC profile

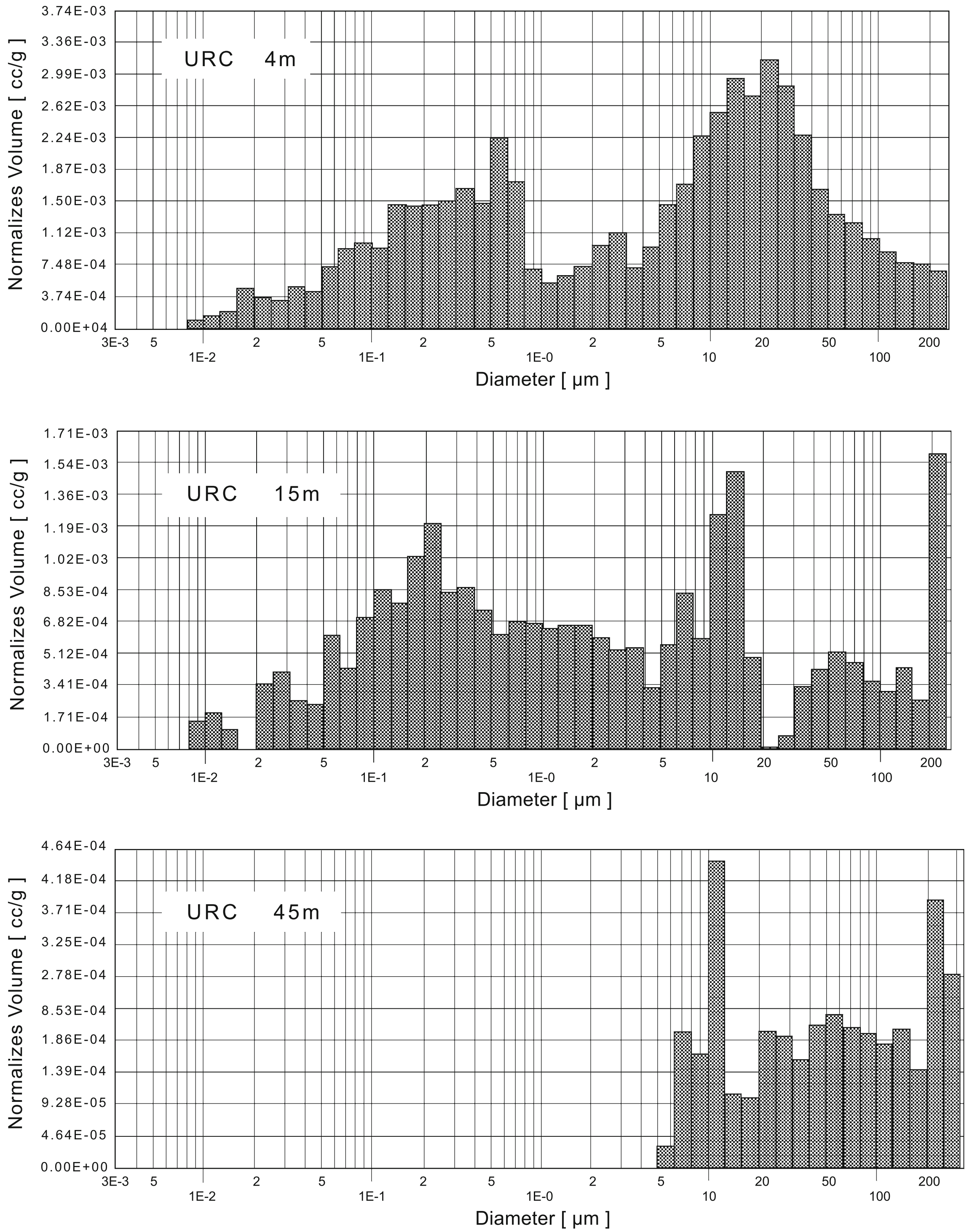

Fig. 8 Changes in pore size distribution in three samples from the URC profile

due to the removal of the Fe oxy-hydroxides from the joint planes just beneath the Raña cover.

As in the previous case, the nitrogen adsorption–desorption isotherms were only useful for samples located at the top of the profile, with a value of ca. 10-11 m^2/gr.

Hydric properties revealed an important reduction in bulk density at the top of the profile (Fig. 9). Total and free porosity (Fig. 10) rapidly widen upwards, but the values for non-free porosity are low throughout the profile. The Hg porosimetry method showed that, except for samples

Table 1 XRD data of both the <2 mm and of the <2 µm fractions of samples from the URC profile

From the Raña bottom	Quartz	Feldspar	Phyllosil.	Oxyhydr.	Phyllosilicates (<2 µm fraction)			
					1:1 group	Illite micas	2:1 group	Interstrat.
Profil URC								
1.5 m	xx	x	xx	t	x	x	x	t
4 m	xx	x	xx	x	x	xx	x	t
15 m	xx	x	x	–	t	x	t	t
35 m	xx	xx	x	–	t	xx	t	–
45 m	xx	xx	x	–				

– Non-detected, *t* traces, *x* frequent, *xx* abundant

Table 2 Chemical data, matter lost, and Parker's index (I_w) of samples from the URC profile

From Raña bottom	$SiO_2 + Al_2O_3/CaO + MgO + Na_2O + K_2O$	$Al_2O_3 + Fe_2O_3/SiO_2$	$K_2O/CaO + MgO + Na_2O$
Profile URC			
1.5 m	14.51	0.24	2.41
4 m	10.82	0.19	1.36
15 m	8.99	0.25	0.60
35 m	8.15	0.26	0.81
45 m	8.26	0.29	0.60

Table 3 Geochemical relationships among the oxides of main components of the URC profile

From Raña bottom	SiO_2%	Al_2O_3%	Fe_2O_3%	MnO%	MgO%	CaO%	Na_2O%	K_2O%	TiO_2%	P_2O_5%	Vol%.	Matter lost%	Parker I_w
Profile URC													
1.5 m ΔCi	71.06	15.37	2.09	0.02	0.38	0.25	1.11	4.20	0.21	0.05	4.26		47
4 m ΔCi	75.42	13.46	1.38	0.03	0.35	0.56	2.57	4.73	0.17	0.14	1.94		65
	+0.90	–4.15	–2.16	–0.03	–1.40	–0.88	–2.66	–0.02	–0.48	–0.16	–0.55	11.4	
15 m ΔCi	69.80	14.95	2.99	0.05	0.89	1.99	3.05	3.49	0.43	0.22	2.75		63
	–2.97	–2.58	–0.68	–0.01	–0.90	+0.43	–0.88	–0.60	–0.27	–0.09	–0.06	8.8	
35 m ΔCi	68.33	14.83	3.44	0.06	2.06	0.47	3.09	4.58	0.43	0.20	2.54		73
	–1.05	–2.04	–0.12	0.00	+0.33	–0.93	–0.71	+0.58	–0.23	0.08	–0.14	4.5	
45 m	66.43	16.17	3.40	0.06	1.17	1.38	3.66	3.78	0.67	0.28	2.56		74

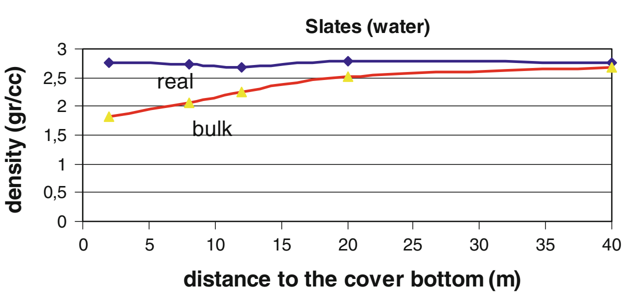

Fig. 9 Changes in real and bulk densities with depth in the SER profile

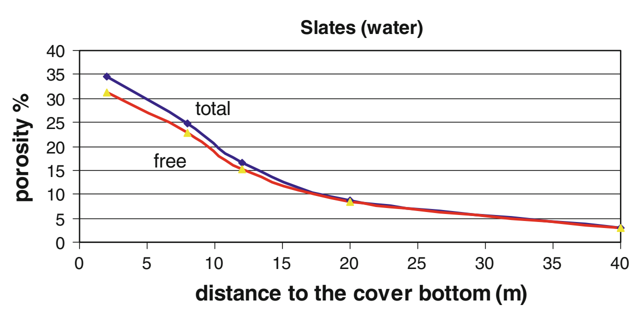

Fig. 10 Changes in total and free porosities with depth in the SER profile

from the base of the profile with a very low specific surface (~0.003 m^2/gr), the rest offered different values with an irregular distribution along it. Nevertheless, samples from the top of the weathered slates showed the highest values, being between 2.3 and 3.6 m^2/gr.

A comparison of data on total porosity obtained by means of the Hg technique on samples of both profiles (Fig. 11) showed that this parameter increases upwards more rapidly in slates. Moreover, the histogram of pore

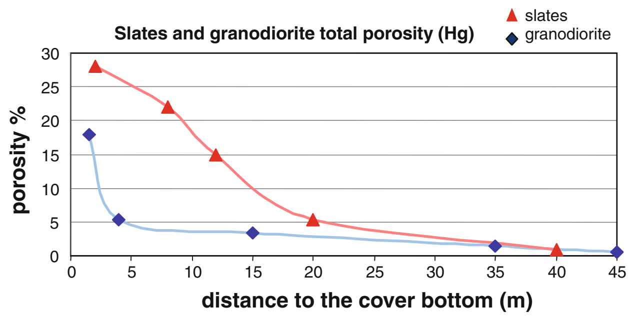

Fig. 11 Comparison of changes in total porosity of the samples from the two profiles studied

size distribution (Fig. 12) confirms that weathering has brought about a selection towards a pore diameter of 1 μm.

The mineralogical data from the profile developed on slates (Table 4) show two features: (1) a slight increase in oxy-hydroxides, in the kaolinite and interstratified groups, with a reduction in feldspars and illite-mica upwards, and (2) the presence of chlorite in the lower levels of the profile. Here too quartz dykes crossing the rock preserve their directions upwards close to the base of the Raña cover, which means that the process of weathering has been more or less conservative in volume.

Both the acid/alkaline and $K_2O/(CaO + MgO + Na_2O)$ fractions (Table 5) point to that some weathering effects begin to appear at ca. 12 m deep. Table 6 shows chemical data and results of the ΔC_i and Parker index of samples from this profile.

Discussion

Generally, weathering can be defined as the sum of processes that affect rocks giving rise to new products and structures that are more stable under the surface environments. Weathering has to be regarded as one of the main processes in the geological cycle as of equal importance as metamorphism, diagenesis, erosion, etc. (Gagny and Cottard 1980; Wilson 2004).

Since the nineteenth century, many studies on rock weathering have been performed, but the number of papers focused on the role of porosity in the process is limited. Authors as Büdel (1957), Boulet (1974), Bocquier et al. (1977), Boulet et al. (1984) Rayot (1994), Twidale and Milnes (1983), Twidale (1962, 2002), Twidale and Bourne (1998) among others, have shown that weathering may continue for very long periods depending on the regional evolution of water tables, climate and tectonism. With the criteria and techniques of the Micromorphology in the last decades (Brewer 1964, 1976; Bullock et al. 1985; Nahon 1991; Delvigne 1998), the methodology of these studies has focused attention to the microenvironments (microsites) where the processes are taking place.

All weathering processes are controlled by three main factors: (1) characteristics of the rock (e.g. grain size, fabric, porosity, mineral and chemical composition), (2) solubility (e.g. ions/molecules present, concentrations, ionic force, acidity, etc.), and (3) environmental factors (e.g. temperature, organic matter, drainage, etc.). All these factors are related to each other, which involves that any variation in one of them leads to changes in the others.

Porosity, both, controls and is affected by weathering. Change in porosity lead to changes in the pattern, distribution and size of pores, in the pore/rock volume ratio, in "specific surface" (m^2/g) and in density (g/cc) of the rock. In general, but not always, increased weathering leads to a reduction in density and an increase in the specific surface. According to this, some authors (Pédro and Delmas 1980; Meunier 1980) have distinguished three systems of weathering: (1) contact microsystems (pore dimensions Å-nm), (2) plasmic microsystems (pore dimensions nm-μm), and (3) fissure system (pores dimensions μm-cm).

In contact microsystems much of the H_2O molecules are not stable and water occurs as OH^- ions attached to the hydroxilated minerals. As weathering progresses, minerals dissolve, change and/or evolve to the clay fraction. Clays give rise to the plasmic microsystem, with high specific surface (e.g. smectites > 150 m^2/gr). Water molecules are stable but they adhere tightly to the pore walls show little or no motion. Under these conditions, diffusion is the main mechanism of weathering (Brady 1990; Pédro 1993; Meunier et al. 2007) leading to the development of particular microenvironments and features (e.g. nodules, pseudogley traits, etc.). When the pore diameter is wider than ca. 1–3 μm, flow begins to be important, and drainage plays a role. Good drainage favours the release and leaching of solutes from the system, while poor drainage leads to stagnant conditions (e.g. generation of evapotites).

This work has focused mainly on two aspects of rock weathering: the evolution of porosity, and the transfer of matter through the weathered material. The parent rocks of the profiles studied have an inherited porosity formed by a network of fissures and fractures defining polyhedra of different sizes and shapes. It is important to note that the porosity studied here is mainly that developed within these polyhedra.

The hydric data (Figs. 7, 10) show that porosity increases upwards in both profiles, the rate being greater in slates than in granodiorite. They also reveal that the real densities of the granodiorite and slates (Figs. 6, 9) have not changed during weathering, while bulk density reduces upwards.

The Hg technique have reported that samples from granodiorite show a total porosity lower than samples from

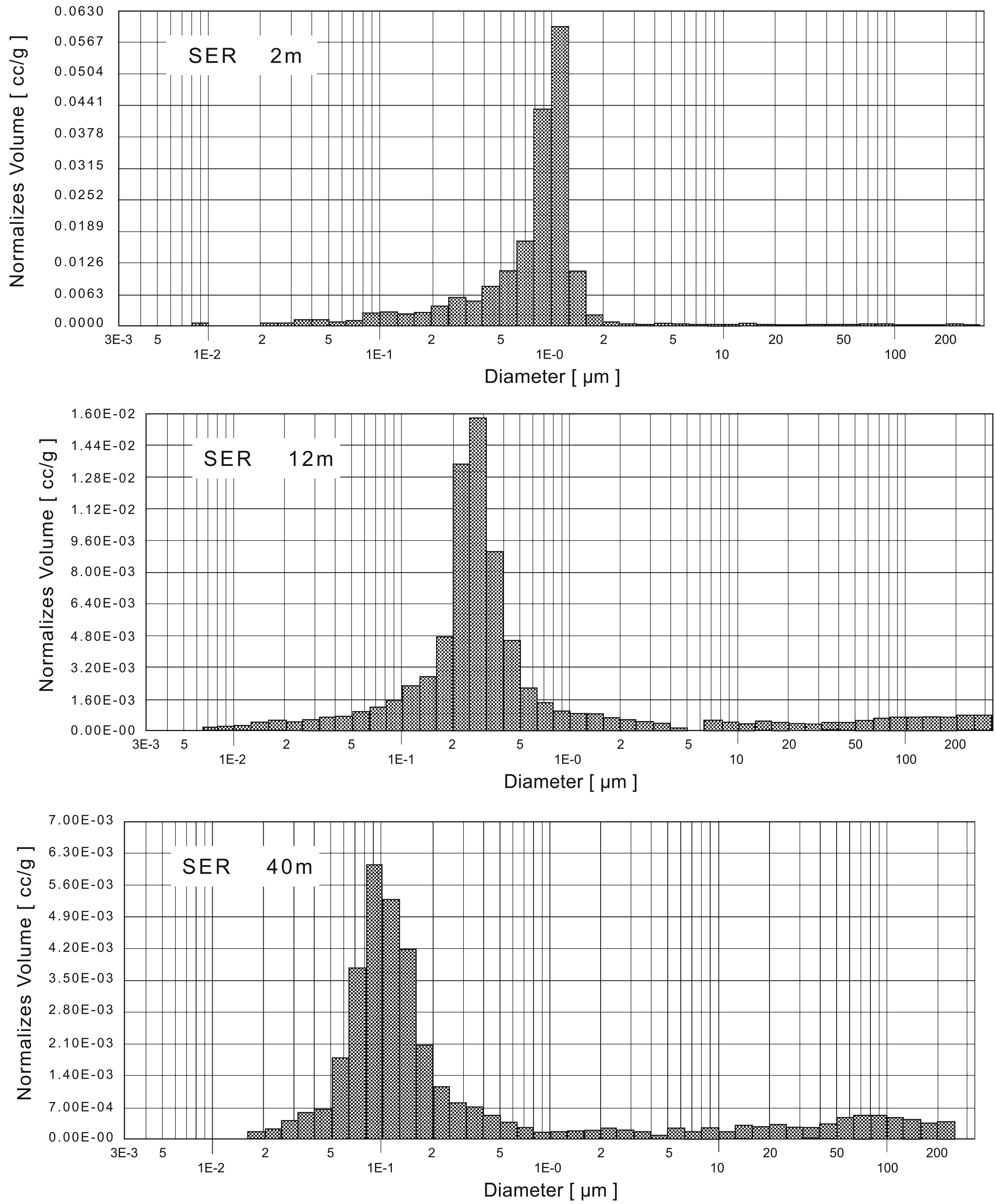

Fig. 12 Changes in pore size distribution in three samples from the SER profile

slates; but comparing the trends of this parameter in the two profiles (Fig. 11), samples from granodiorite show a marked increase close to the cover bottom. It may be related to an increase in the clay content within the saprolithe. Moreover, in the granodiorite the Hg porosimetry (Fig. 8) shows that weathering has caused a fine porosity with a pore diameter <5 µm, while it has led to a selective porosity of ca. 1 µm in slates (Fig. 12). Therefore, the behaviour of the trapped water will be different in the two profiles (Figs. 7, 10).

Porosities of ca. 1 µm establish the difference between flow and the absence of flow of water through the fine pores (Pédro and Delmas 1980; Pédro 1993). In these two profiles, some water is retained within the fine pores of the weathered rock, being slightly higher on slates (ca. 5%) than in granodiorite (ca. 3.5%). Once into the pores, it is

Table 4 XRD data of both the <2 mm and of the <2 μm fractions of samples from the SER profile

From the Raña bottom	Quartz	Feldspar	Phyllosilicates (<2 μm fraction)	Oxyhydr.	1:1 group	Illite micas	2:1 group	Chlorite	Interstr..
Profile SER									
2 m	xx	t	xx	x	xx	x	x	–	x
8 m	xx	x	xx	t	x	x	x	t	x
12 m	xx	x	xx	t	t	xx	x	t	t
20 m	xx	xx	xx	–	t	xx	t	x	t
40 m	xx	xx	xx	–					

– Non-detected, *t* traces, *x* frequent, *xx* abundant

Table 5 Chemical data, matter lost, and Parker's index (I_w) of samples from the SER profile

From Raña bottom	$SiO_2 + Al_2O_3/CaO + MgO + Na_2O + K_2O$	$Al_2O_3 + Fe_2O_3/SiO_2$	$K_2O/CaO + MgO + Na_2O$
Profile SER			
2 m	20.08	0.47	5.08
8 m	13.95	0.43	2.09
12 m	11.22	0.40	1.01
20 m	9.66	0.41	0.87
40 m	9.40	0.42	0.87

Table 6 Geochemical relationships among the oxides of main components of the SER profile

From Raña bottom	SiO_2%	Al_2O_3%	Fe_2O_3%	MnO%	MgO%	CaO%	Na_2O%	K_2O%	TiO_2%	P_2O_5%	Vol%.	Matter lost%	Parker I_w
Profile SER													
2 m ΔCi	60.80	21.14	7.52	0.01	0.65	0.02	0.00	3.41	0.40	0.09	6.72		32
	−18.64	−4.84	−1.41	−0.06	−2.45	−0.27	−1.32	−1.65	−0.11	−0.13	+0.04	30.85	
8 m ΔCi	60.02	18.70	7.32	0.16	1.84	0.01	0.02	3.77	0.40	0.13	6.20		37
	−9.16	−3.33	−0.32	+0.07	−1.36	−1.26	−1.32	−0.77	−0.04	−0.08	+0.93	15.4	
12 m	62.94	17.95	7.57	0.08	3.15	0.17	0.27	3.62	0.56	0.11	4.75		40
ΔCi	−6.74	−3.97	−0.12	−0.02	−0.30	−0.15	−1.09	0–95	+0.10	−0.10	−0.29	14.0	
20 m	60.42	18.52	6.54	0.06	2.84	0.25	1.26	3.82	0.88	0.16	3.85		50
ΔCi	−2.71	−1.61	−0.30	0.00	−0.23	−0.04	−0.13	−0.35	+0.44	−0.03	−0.64	5.7	
40 m	59.18	18.92	6.42	0.06	2.89	0.28	1.31	3.92	0.38	0.19	4.24		62

retained as non-movable water, the rest of which being leached out throughout the fissures and cracks. According to Figs. 8 and 12, diffusion can affect the whole profile on slates due to the fine pores, whereas in the profile on granodiorite the effects occur higher in the profile, where pores finer than <5 μm appear.

In both profiles, weathering has led to important transformations in the mineralogical composition, with the generation of some 2:1 and 1:1 phyllosilicates, and oxyhydroxides as new minerals (Tables 1, 4). At the top of the profile on slates, just beneath the Raña cover, Fe ions released by weathering are oxidized, most of them remaining in situ and giving rise to the red hues of this level. Only along the immediate walls of fissures and fractures, where flow is possible, do the hues change to yellowish, greyish, and even whitish, mainly depending on the chemical and/or biochemical conditions of the solutions. These changes in colour are due to the degree of hydration of the oxyhydroxides which is also controlled by the pore space (Tardy and Nahon 1985; Nahon 1991): the finer are the pores the more dehydrated (more reddish) are the oxyhydroxides.

Some of the most interesting results obtained concerns the movement of components through the weathered rocks.

Using the Grant's Equation (1) in both profiles, it may be seen that practically all elements are mobile (Tables 3, 6): slates have released ca. 30%, and granodiorite at least ca. 12%, without taking into account the upper part of the profile. This means that at the top of the profiles, slates have lost up to ca. 800 kg/m^3 of matter and granodiorite more than 300 kg/m^3. Moreover, these tables also show that Parker's index affords a higher value in granodiorite than in slates. According to this index, the slates (lower index) should be more resistant than the granodiorite (higher index). However, the difference between the two extremes in both profiles is higher on slates than on granodiorite, which means that slates have also undergone a higher degree of weathering.

On the other hand, the geochemical indices (Tables 2, 5) outline that in both profiles the weathered basement presents a lower and an upper part, the separation being located between 4 and 15 m deep in the URC profile, and between 12 and 20 m deep in the SER profile. Taking into account that K ions are common in quite resistant silicates as muscovite and microcline, and that in our profiles the content in feldspar reduces upwards, the source of this element will be mainly the micas and interstratified phyllosilicates.

After the data of Tables 3 and 6, Al, Fe and Na appear as the main elements lost in samples from the granodiorite, whereas Si and Al are the main elements lost in samples from slates. By contrast, data after Tables 2 and 5 point that Si, Al and K are concentrated upwards in both profiles. In the profile on granodiorite this apparent contradiction can be explained due to that many of the dissolved minerals are plagioclase and biotite which deliver a lot of Si, Al, Na, Ca, Fe, etc. to the solution. Minerals as muscovite, quartz and part of the K feldspar remain in a regolith lighter in density but preserving the parent structures. By contrast, in the profile on slates the resistant minerals, apart of quartz, will be K phyllosilicates (e. g. muscovites more or less weathered and vermiculites) while most of feldspars are weathered due to their small grain size.

The $(Al_2O_3 + Fe_2O_3)/SiO_2$ fraction is used also to evaluate the climatic and/or geomorphological meaning of these profiles. According to Tables 2 and 5, there are not drastic changes in this relationship through the profiles. But a typical feature of the tropical and subtropical soils is the enrichment in 1:1 phyllosilicates (mainly kaolinite) and Fe oxyhydroxides at the top of the profiles, and here this enrichment has not any significance except, perhaps, in the profile on slates. Therefore, according to mineralogical and chemical data, and to the different indices used here, weathering affecting the basement looks like to be better related to the hydrological evolution of the landscape than having any climatic significance (Molina Ballesteros and Cantano Martín 2002). For a very long time (at least since the Pliocene to the lower Pleistocene?) the basement underwent weathering processes under groundwater conditions, as long as water tables were close to these piedmont surfaces. Once the drainage systems start to insert into the landscape, water tables went down leading to the weathering mantle outcrops. Where the Raña cover is not thick (e.g. <3–4 m) pedological and hydrogeological weathering can contact each other, and the limit between the two processes is difficult to establish due to the removal of mater.

This protracted removal of matter from both the profiles and the landscapes has important consequences. It leads to subsidence and compaction of sediments (e.g. ponds on the Raña surface) and, with time enough, to unequal volume reductions with the reinforcement of differences in the reliefs (Twidale, 2007).

The two profiles studied here are located not far from the headwaters of their landscapes, such that they are zones where leaching is dominant. Under geological stability for a very long time, the loss of matter has led to a lowering of the landscape in a fairly homogeneous way, giving rise to well levelled piedmont platforms and hills with gentle slopes. Currently, the profiles continue to evolve, as seen in their persistent humidity even during dry seasons.

Conclusions

The present work emphasizes the importance of changes in porosity for the rock weathering. Variations in this parameter have had significant consequences in the mineralogical and geochemical processes studied.

At the same time, weathering has given rise to changes in pore size distribution within the profiles: it has created a fine porosity of <5 μm in diameter on granodiorite, but leading to a selective porosity of *ca*. 1 μm in diameter on slates.

Changes in porosity and bulk density (hydric properties) are related to mineralogical variations and the movement of matter within the profiles. According to the Grant's equation, almost all major elements are moved, either in solution or carried away within the leached minerals. Assuming that most of the weathering is isovolume, this loss of matter can reach up to ca. 800 kg/m^3 in slates, and may exceed the 300 kg/m^3 in granodiorite in the upper levels of the profiles studied.

These changes are also related to the generation of new minerals such as phyllosilicates of the smectite *s.l.* and kaolinite *s.l.* groups and Fe oxy-hydroxides. Smectites appear in the intermediate level of the weathering in both profiles while kaolinites lead to be dominant at the top of the profiles.

There have been two types of weathering working at the same time: (1) hydrogeological weathering, affecting to the basement and being more or less conservative for the inherited structures, and (2) pedological weathering, which disturbed the inherited structures affecting to the Raña sediments and to the upper part of the basement.

All these weathering processes are related to the morphological evolution of the region, at least since the Upper Neogene period, most of them are still active. They have led to a long-term lowering of the landscape, giving rise to levelled piedmont platforms and gentle hillside slopes. They have the potential to explain topographic features in terms of bedrock porosity and susceptibility to weathering, and also to the development of various specific land forms and to landscape evolution.

Acknowledgments The authors acknowledged the interesting suggestions of Prof. C. R. TWIDALE. We also thank the Ministerio de Educación y Ciencia of Spain and the Junta de Castilla y León for financial support under Projects CGL2007-62168/BTE (funds FEDER) and Project SA024A07, respectively.

References

Baumgartner LP, Olsen SN (1995) A least-squares approach to mass transport calculations using the isocon method. Econom Geol 90:1261–1270

Birot P, Solé Sabaris L (1954) Investigaciones sobre la morfología de la Cordillera Central española. Nsto J S Elcano CSIC, Madrid, p 87

Bocquier G, Rognon P, Paquet H, Millot G (1977) Géochimie de la surface et formes du relief. II. Interpretation pédologiques des depressions annulaires entourant certains inselbergs. Sci Géolog Bull 30(4):245–253

Borger H (1997) Enviromental changes during the Tertiary: the examples of palaeoweathering residues in Central Spain. In: Widdowson M (ed) Palaeosurfaces: recognition, reconstruction and palaeoenviromental interpretation. Geological Society of London Special Publication n° 120, pp 159–173

Boulet R (1974) Toposéquences de sols tropicaux en Haute Volta. Equilibres et déséquilibres pédobioclimatiques. Thèse Sci, Strasbourg, p 330

Boulet R, Chauvel R, Lucas Y (1984) Les systemes de transformation en Pédologie. In: *Livre Jubilaire du Cinquantrnaire 1934–1984*, Association Française pour l'Étude du Sol (AFES), 167–179

Brady NC (1990) The nature and properties of Soils, 10th edn. MacMillan, New York, p 621

Brewer R (1964) Fabric and mineral analysis of soils. Wiley, New York, p 462

Brewer R (1976) Fabric and mineral analysis of soils. Robert E. Krieger Pub. Co, Huntinton, p 482

Brimhall GH, Lewis CJ, Ford C, Bratt J, Taylor G, Waring O (1991) Quantitative geochemical approach to pedogenesis: importance of parent material reduction, volumetric expansion and eolian influx in laterization. Geoderma 51:51–91

Büdel J (1957) Die "Doppelten Einebnungsflächen" in den fauchten Tropen. Zeitschrift für Geomorphologie, NF 1:201–228

Bullock P, Fedoroff N, Jongerius A, Stoops G, Tursina T, Babel U (1985) Handbook for soil thin sections description. Waine Research Publ, Albrighton, p 152

Cantano Martín M, Molina Ballesteros E (1999) La cuenca de Ciudad Rodrigo y sus bordes. Studia Geol. Salmanticensia, vol esp. N° 7: La evolución del relieve en zócalos antiguos. Procesos, formaciones superficiales y sedimentos asociados. Salamanca, pp 121–135

Chiquet A, Colin F, Hamelin B, Michard A, Nahon D (2000) Chemical mass balance on the Toledo granite (Spain). Chem Geol 170:19–35

Clausell JV, Bastida J, de la Torre J, Ramo P (2001) Balance de masas en procesos de alteración sobre pizarras paleozoicas del Macizo Ibérico. Actas III Congr. Ibérico de Geoquímica y VIII Congr. Geoquímica de España, Zaragoza, pp 347–350

Delvigne JE (1998) Atlas of micromorphology of mineral alteration and weathering. Canadian Miner Specl Publ 3:494

Espejo R (1978) Estudio del perfil edáfico y caracterización de las superficies tipo Raña del sector Cañamero- Horcajo de los Montes. Tesis Doctoral ETS Ingenieros Agrónomos, Madrid. 477 pp (Unpublished)

Espejo R (1987) The soils and ages of the "Rañas" surfaces related to the Villuercas and Altamira mountain ranges (Western Spain). Catena 14:399–418

French Standard Norm NF B10 (1973) Mesures de la porosité, de la masse volumetrique réel et de la masse volumetrique apparente, Paris 503

French Standard Norm NF B10 (1973) Mesure du Coéficient d'Absorption d'Eau, Paris 504

Gagny C, Cottard F (1980) Proposition de signes conventionnels pour la répresentation de certaines structures magmatiques acquises au course de la mise en place et de la cristallisation. Comptes Rendus 105ième Congrès National de la Societé de Savantes, Caen (Sciences), vol 2, pp 37–50

Gallardo J, Pérez González A, Benayas J (1987) Paleosuelos de los pidemontes villafranquienses y de las terrazas pleistocenas de la región de valle de Henares- Alto Jarama. Boetín Geológico y Minero 98:27–39

García Rodríguez MP (1987) Dinámica del hierro y del aluminio en suelos desarrollados sobre sedimentos pliocenos del Campo de Yeltes (Salamanca). Trabajos del Centro de Edafología y Biología Aplicada (CSIC), Salamanca, p 98

García Rodríguez MP, Corteza Bonin J, Sánchez Camazano M, Prat Pérez L, Lorenzo Martín LP, Ledesma García M (1977) Suelos sobre sedimentos postmesozoicos de la zona Yeltes-Huebra (Salamanca). Anuario del Centro de Edafología y Biología Aplicada (CSIC), Salamanca, pp 107–139

Gladfelter BG (1971) Meseta and Campiña landforms in Central Spain. A geomorphology of the Alto Jarama basin. The University of Chicago. Dept. of Geography, Research Paper n° 130, pp 204

Grant JA (1986) The Isocon diagram. A simple solution to Gresens' equation for metasomatic alteration. Econ Geol 81:1976–1982

Ingelmo F, Cuadrado S, Hernández J, Ibáñez A (1991) Degradación física de los suelos de una zona de Rañas de la provincia de Salamanca. Suelo y Planta 1:619–630

Martín Serrano A (1988) El relieve de la región occidental zamorana. La evolución morfológica de un borde del Macizo Hespérico. Insto. de Estudios Zamoranos "Florián de Campo", CSIC-Diputación de Zamora (eds), pp 309

Martín Serrano A (1991) La definición y el encajamiento de la red fluvial actual sobre el Macizo Hespérico en el marco de la geodinámica alpina. Rev Soc Geol España 4:337–351

Martínez Lope MJ, García González MT, Molina Ballesteros E (1995) Relationship between geomorphology and palaeoweathering on the Hercynian basement in Central Spain: a mineralogical and geochemical approach. Rev Soc Geol España 8:127–136

Meunier A (1980) Les mécanismes de l'altération des granites et le rôle des microsystèmes. Étude des arènes du Massif granitique de Parthenay (Deux-Sèvres). Mém Soc Géol France 140:1–80

Meunier A, Sardini P, Robinet JC, Pret D (2007) The petrography of weathering processes: facts and outlooks. Clay Miner 42:415–435
Molina Ballesteros E, Cantano Martín M (2002) Study of weathering processes developed on old piedmont surfaces in Western Spain: new contributions to the interpretation of the “Raña” profiles. Geomorphology 42:279–292
Molina E, Cantano M, Vicente MA, García Rodríguez P (1990) Some aspects of palaeoweathering in the Iberian Hercynian Massif. Catena 17:333–346
Molina E, García González MT, Espejo R (1991) Study of paleoweathering on the Spanish Hercynian basement. Montes de Toledo (Central Spain). Catena 18:354–354
Nahon DB (1991) Introduction to the petrology of soils and chemical weathering. Wiley, New York, p 313
Pardo E, Gallardo J, Pérez-González A, Gómez-Miguel V (1993) Variabilidad morfológica de suelos en el piedemonte de la Raña de la vertiente norte de Montes de Toledo. In: La Raña en España y Portugal, Monografía n° 2 del Centro de Ciencias Medioambientales, C.S.I.C., Madrid, pp 149–157
Parker A (1970) An index of weathering for silicate rocks. Geol Mag 107:501–504
Pedraza J (1978) Estudio geomorfológico de la zona de enlace entr las Sierras de Gredos y Guadarrama (Sistema Central español). Tesis doctoral, Fac. Ciencias Geológicas, Univ. Complutense, Madrid (unpublished)
Pédro G (1993) Un phénomène normal de la surface de la planete : l’alteration des roches. In: Vicente Henández MA, Molina Ballesteros E, Rives Arnau V, CSIC (eds) Alteración de granitos y rocas afines. Madrid, pp 17-50
Pédro G, Delmas AB (1980) Regards actuels sur les phénomènes d’alteration hydrolitique. Cahiers ORSTOM, (Pédologie) 18(3–4):217–234
Portero JM, Aznar JM (1984) Evolución morfotectónica y sedimentación terciarias en el Sistema Central y cuencas limítrofes (Duero y Tajo). I Congreso Español de Geología. Tomo 3:253–263
Rayot V (1994) Altérations du centre de l’Australie: rôle des solutions salines dans la génèse des silcretes et des profiles blanchis. *Mémoires Sciences de la Terre*, 22, École de Mines de Paris-CSIRO Australia, 142 pp
Reiche F (1943) Graphic representation of chemical weathering. J Sediment Petrol 13:58–68
Ribeiro O (1942) Notas sobre a evolucao geomorfológica da orla meridional da Cordilheira Central entre Sobreira Formosa e a fronteira. Bol Soc Geol Portugal 1:123–144
Rives V (1990) Computer program for analyzing nitrogen adsorption isotherms on porous solids. Absorp Sci Technol 8:95–103
Solé Sabaris L (1952) Geografía de España y Portugal. Tomo 1. España. Geografía Física: El Relieve. Montaner y Simon, Barcelona, p 500
Swenzner JE (1936) Zur morphologie des Zentral Spanischen Hochlandes. Geographie Abhandel 3(10):128
Tardy Y, Nahon D (1985) Geochemistry of laterites. Stability of Al-goethite, Al-hematite and Fe^{3+}-kaolinite in bauxites and ferricretes. An approach to concretion formation. Am J Sci 285:865–903
Twidale CR (1962) Steepened margin of inselbergs from north-western Eyre Peninsula, South Australia. Zeitschrift für Geomorphologie 6(1):51–69
Twidale CR (2002) The two stage concept of landform and landscape development involving etching: origin, development and implication of an idea. Earth Sci Rev 57:37–74
Twidale CR (2007) Concatenation and resultant inequalities in denudation. Phys Geogr 28:50–75
Twidale CR, Bourne JA (1998) Flared slopes revised. Phys Geogr 19(2):110–133
Twidale CR, Milnes AR (1983) Slope processes active late in arid scarp retreat. Zeitschrift für Geomorphologie 27(3):343–361
Vaudour J (1977) *La* region de Madrid. Alterations, sols et paléosols. Thése Doctorat d’État, Ed. Ophris, 1979, pp 390
Vicente MA, Molina E, Espejo R (1991) Clays in paleoweathering processes: study of a typical weathering profile in the Hercynian basement in the Montes de Toledo (Spain). Clay Miner 26:81–90
Vicente MA, Elsass F, Molina E, Robert M (1997) Paleoweathering in slates from the Iberian Hercynian Massif (Spain): investigation by TEM of clay mineral signatures. Clay Miner 32:435–451
Wilson MJ (2004) Weathering of the primary rock-forming minerals: processes, products and rates. Clay Miner 39:233–266